Ab Initio Investigation on the Thermoelectric Properties of γ-CuI for Thermoelectric Device Applications

R. Vettumperumal[1*], R. Thangavel[2], S. Kalyanaraman[3]

[1]Department of Physics, Fodhdhoo School, Noonu Atoll, Republic of Maldives – 04120.
[2]Department of Applied Physics, Indian Institute of Technology, Dhanbad, India - 826004.
[3]Sri Paramakalyani College, Alwarkurichi, Tamil Nadu, India – 627425.
*Correspondence to: R. Vettumperumal,e-mail: vettumperumalphy@gmail.com.

Abstract: *Semi-classical transport thermoelectric properties of γ-CuI are investigated using density functional theory (DFT) calculation containing Boltzmann transport equations. The Tran–Blaha modified Becke–Johnson potential (Tb-mBJ) approximation is used as the exchange correlation potential. Thermoelectric properties such as, Seebeck co-efficient, electrical conductivity, thermal conductivity, power factor, figure of merit, thermoelectric voltage and thermoelectric conversion efficiency are discussed with constant relaxation time as a function of chemical potential. This is because the chemical potential is directly related with the carrier concentration and temperature. These parameters are strongly dependent on the doping level and temperature. The maximum range of figure of merit (0.8 – 1.0) and conversion efficiency (93%) is found to be in the range of chemical potential.0.032 – 0.036 Ry. The active thermoelectric region of γ-CuI is observed in the range of temperature from 300 K to 450 K. Hence, γ-CuIbehaves excellent thermoelectric material for heat generation and extraction applications.*

Keywords: *Copper Iodide; Density functional theory; thermoelectric properties; chemical potential.*

I. Introduction

Nowadays, the usages of plentiful heat sources (consumer electronics, solar cells, home heater and wearable devices) innear room temperature is tremendously reside in day to life. Harvesting of such energyfrom room temperature range devices has significant interest in the scope of present researchers. Agood thermoelectric material such as heavily doped semiconductors have an energy band gap value (E_g) close to 0.4 eV[1]. Mostly established thermoelectric materials have a tendency to be optically opaque because of their small band gap [2, 3]. Recently, quite a lot ofcategories of non-transparent thermoelectric materials such as tellurides[4], half-Heuslers[5] and silicides[6]were reported with attractive thermoelectric properties for renewable power generation applications. Few optically transparent ($E_g > 3\ eV$) thermoelectric devices are known to exist till now, which could be open a new field of novel applicationsin smart windows (or screens), cooling and thermal sensors. In addition to these, it is the fast on-chip cooling and power recovery [7, 8]in optoelectronic devices together with solar cells, infrared photo detectors, as well as fully transparent electronic devices.

Transparent thermoelectric material ismostlybeing gooda transparent conductor (TC) with high *S* and low *k*values.*N-* and *p*-type transparent thermoelectric materials are indispensable to manufacture the thermoelectric device. However, the deficiency of highly conductive *p*-type TCs leads to the recent research has focused on thermoelectric properties of *n*-type TCs including heavily doped ZnO[9] In$_2$O$_3$[10] and SrTiO$_3$[11]. Among these *n*-type TCs, Sn-doped In$_2$O$_3$ (ITO) shows the highest value of figure of merit (ZT) ~ 0.14 at room temperature. Conversely, *p*-type TCs usually exhibit poor electrical conductivities, which is leading to poor thermoelectric performance at room temperature, for example, ZT ~ 0.001 for CuAlO$_2$[12] and ZT ~ 0.002 for CuCrO$_2$[13]. The p-type misfit-layered oxide Ca$_3$Co$_4$O$_9$ was possessing thermoelectric performance (ZT ~ 0.07 at room temperature for single crystal) comparable to the *n*-type TCs.But, it is not exactly transparent due to its small band gap (E_g ~ 2.1 *eV*) value[14]. Therefore, the lack of *p*-type transparent thermoelectric materials is the foremostimpediment in comprehension of fully transparent thermoelectric devices.

Beginning of 1907, transparent conducting properties of zincblende copper iodide (CuI)was exposed by Bädeker[15, 16]. The wide direct bandgap value of CuI (3.1 *eV* at room temperature) leads to a high transparency in the visible spectral range and it hasexciton binding energy (62 *meV*) is similar to that of ZnO[17]. Result of copper vacancies and small effective mass (0.30m_0) of the light holes,CuIhas a native p-type conductivity with high hole mobility (>40 $cm^2V^{-1} \cdot s^{-1}$ in bulk) [18]. It might be possible to improve the hole

conductivity further by appropriate iodine doping [19]. Moreover, n-type doping is alsofeasible in Zn-doped CuI[20, 21], which would be greatly extend its applications.

High room-temperature hole conductivity ($\sigma > 280\ S\ cm^{-1}$) of CuI thin film has been achieved very recently [22]. A large Seebeck coefficient of γ-CuI ($S=237\ \mu V K^{-1}$for a hole concentration p of $10^{20} cm^{-3}$) was theoretically predicted based on the Boltzmann transport theory combining with first-principles calculations at 300 K [23]. Yang *et al*[1] reportedthat the superior thermoelectric performance of transparent p-type γ-CuI thin films in room temperature range. The thermoelectric transport properties of γ-CuI are analyzed based on the single band model. Besides, a prototype of γ-CuI-based transparent and flexible thermoelectric module is demonstrated. However, a detailed study of thermoelectric performance of γ-CuI is in need considering all these aspects. We report here the thermoelectric transport properties of γ-CuI through Boltzmann transport equations using TB-mBJ first principle calculations. Thermoelectric parameters such as, Seebeck co-efficient, thermal conductivity, electrical conductivity, figure of merit and power factors are discussed as a function of chemical potential.

II. Computational details

We have used the first-principle study based on density functional theory with the full-potential linearized augmented plane-wave (FP-LAPW) method for the present study. It is implemented in the WIEN2K package[24]. The exchange and correlation energy have been described by the generalized gradient approximation GGA [25] for structural calculations, and the TB- mBJ approximation [26] for the transport proprieties calculations. All other computational parameter values of γ-CuI used for the present calculation is taken from our previous reported work [27].

The transport properties (Seebeck co-efficient, electrical conductivity, thermal conductivity, power factor and figure of merit)of γ-CuI were calculated using the BoltzTraP code [28] that solvesthe semi-classical Boltzmann transport equation under theconstant relaxation time (τ) approximation and the rigid band approach [29]. One of the shortcomings of the semi-classic Boltzmann equation is that it couldn't describe exactly the carrier scattering mechanisms in a solid. For this reason, the relaxation time approximation is adopted to overcome such complexity, where the relaxation time is treated as an energy independent constant. These approaches have been demonstrated to be a reasonable good approximation for evaluating the optimal doping level of several bulk thermoelectric materials [30-32].

III. Results and Discussions

The electronic band structure near the valance band maximum (VBM) largely describes the thermoelectric performance of materials. Seebeck co-efficient of a material has been enhanced by the flat band at VBM due to a large effective mass. Furthermore, the occurrence of a more dispersive band at VBM leads to the lighter effective mass, which implies high mobility and hence, a larger value for the electrical conductivity. Therefore, a favourable situation for a better thermoelectric performance is the combination of light and heavy bands at VBM [33].

The density of states (DOS) and band structure (inset figure) of γ-CuI is shown in **Fig.1**. Inset figure shows that the γ-CuI phase has less dispersive flat bands and more dispersive parabolic bands. Hence, this may lead to the higher value of thermoelectric power factor. Fig.1 shows that the VBM comprises of Cu and I state. It reveals that the Cu states at VBM come from *3d* orbitals, whereas I state at VBM due to the *5p* orbitals. This result is well accordance with the previous DFT [34] and tight binding approximation calculations [35]. The peak in the DOS of the topmost valence band is situated about 1 *eV*below VBM. It is very much closer to the other *p*-typethermoelectric materials. The closer peak in the VBM shows better thermoelectric performance [36]. Hence, γ-CuIappears to be a comparable thermoelectric material with the other p-type thermoelectric materials.
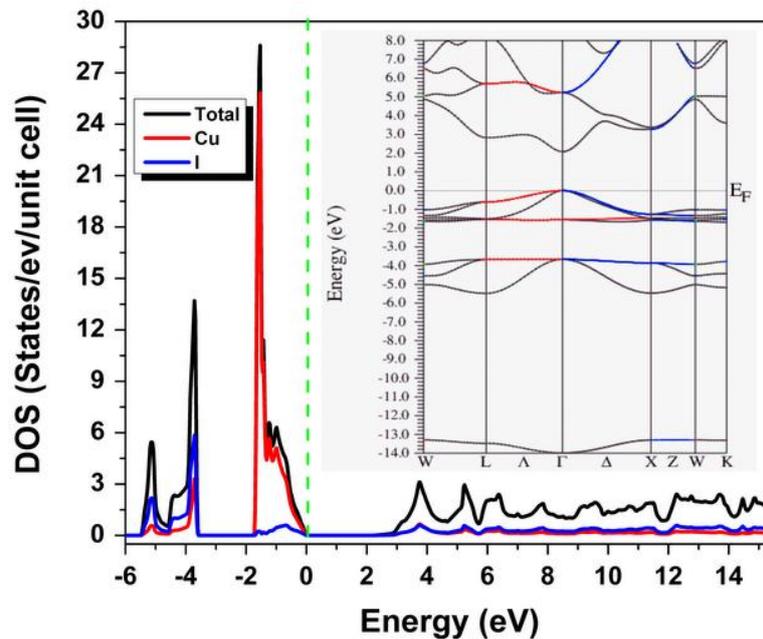
Fig.1: Density of states of γ-CuI, Inset: Band structure of γ-CuI.

The efficiency of thermoelectric device is characterized by a material dependent figure of merit[37],

$$ZT = S^2 \sigma T/K \qquad \ldots\ldots\ldots\ldots.. (1)$$

where, $S^2 \sigma T$ is the thermoelectric power and K is the thermal conductivity. Ioffe*et al*[38] reported that the carrier concentration needs to be optimized in order to obtain the best balance between thermoelectric power and conductivity in a given semiconductor system. A variety of materials with ZT~1 have been discovered over the years with such an optimization.

In order to achieve this optimization, the thermoelectric properties of the materials are analysed as a function of chemical potential (μ). It is the main driving force for any mass transfer operation to occur. It determines the centre of the Fermi – Dirac distribution function, which gives the chemical potential as a function of temperature for a given carrier concentration. Hence, the calculated thermoelectric properties are discussed based on chemical potential, because temperature and carrier concentration are simultaneously optimized through chemical potential.

The position of chemical potential plays decisive role with regard to the transport properties. Chemical potential indicates the doping level (or carrier concentration) of the systemwithin the rigid band picture [29]. It is positive ($\mu > 0$) for *n*-type doping while negative ($\mu < 0$) for *p*-type doping. Hence, the behaviour of chemical potential with varying temperature is important for selection of the proper doping element for increasing thermoelectric response. Chemical potential as a function of temperature is presented in **Fig.2**. It indicates that the *p*-type doping increases with the increase of temperature while the *n*-type doping decreases. It is observed that the hole concentrations are crossing the Fermi level at and above the room temperature (300 K) to 400 K and saturate at above 500 K with
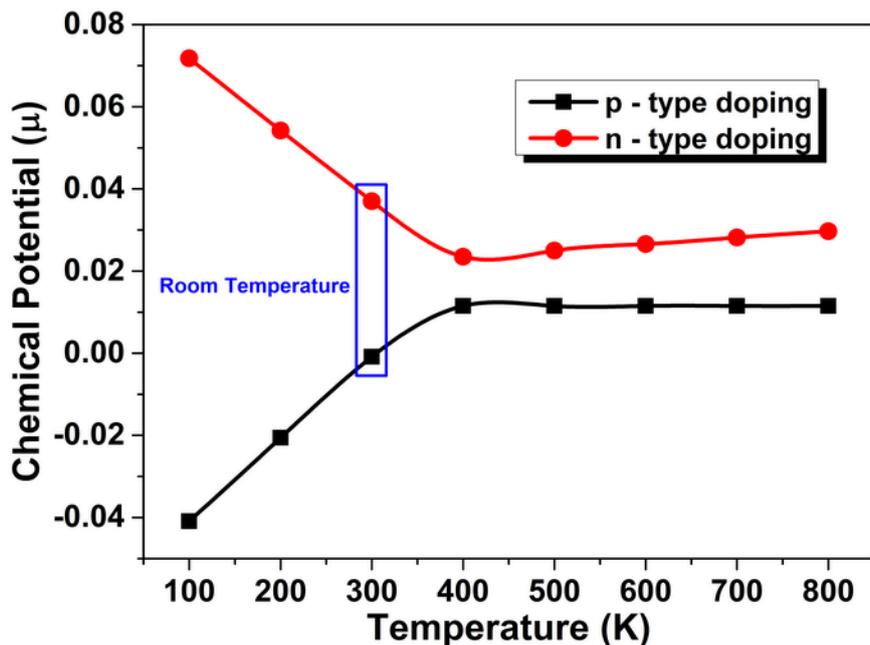
Fig.2: Chemical potential as a function of temperature.

the chemical potential of 0.0115 Ry. It is clearly depicted that the γ-CuI have maximum thermoelectric response around 300 – 400 K temperature range.

Seebeck co-efficient analysis gives information about the optimization of TE performance of the materials. The variation of Seebeck co-efficient with chemical potential is shown in **Fig.3**. It exhibits a single peak pattern along both sides of chemical potential. It is due to the presence of bipolar conduction as expected from the substantial band gap. Fig.3 clearly depicted that at $\mu = 0$, the value of Seebeck co-efficient is 2.88 *mV/K* at 300 K. It confirms the p-type semiconductor nature, as Seebeck co-efficient has greater value at zero chemical potential. **Fig.3** shows that the Seebeck co-efficient decreases with the increase of temperature above room temperature (RT), whereas much more changes are not observed in the peak height at below RT. But the peak position is shifted towards higher chemical potential region.
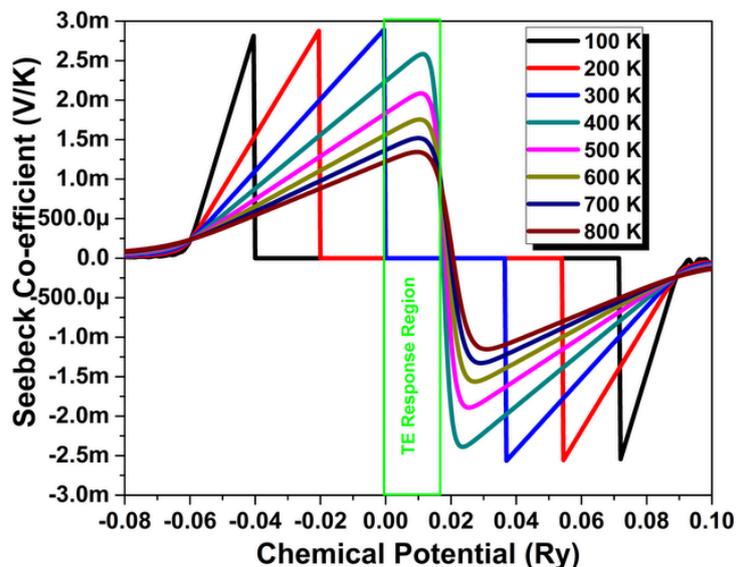
Fig.3: Variation of Seebeck coefficient with chemical potential.

The decreases of Seebeck co-efficient with increase of temperature indicate the presence of compensation between holes and electrons. And also, it can be described by the excitation of electron – hole pairs across the energy gap [39]. This result is concordant to that seen in the case of low band gap TE materials such as PbTe[40]. The values of Seebeck co-efficient are larger than those of PbTe (100 *μV/K*) at RT [41, 42]. Nishikawa *et al*[43] reported that the molten CuI has the value of Seebeck co-efficient lies in the range 620 –

890 $\mu V/K$ for the 880 – 1173 K temperature range. The present calculated Seebeck co-efficient value of γ-CuI is 962$\mu V/K$ at 800 K and it is agreeable to the previously reported experimental results. Seebeck co-efficient is observed around 1 – 2.8 mV/K in the 100 – 700 K temperature range. Thus, the large value of Seebeck co-efficient of γ-CuI is attributed to a large effective mass which is dominated by the heavy hole band. Hence it is desired for efficient TE devices. However, a small difference found between the experimental and theoretical values.

The obvious reason for the difference between the calculated and experimental result is as follows (i) DFT produce results after the materials are optimized at the ground state, while the experimental results are not obtained from the ground state (ii) Pseudo – Eigen values are available in the DFT approximation. The active TE response region of γ-CuI observed from μ = 0 – 0.0178 Ry over the RT to 800 K. The intrinsic character of the semiconductor nature of γ-CuI is observed from the rapid drop in the Seebeck co-efficient values which changes as **1/T**[44].
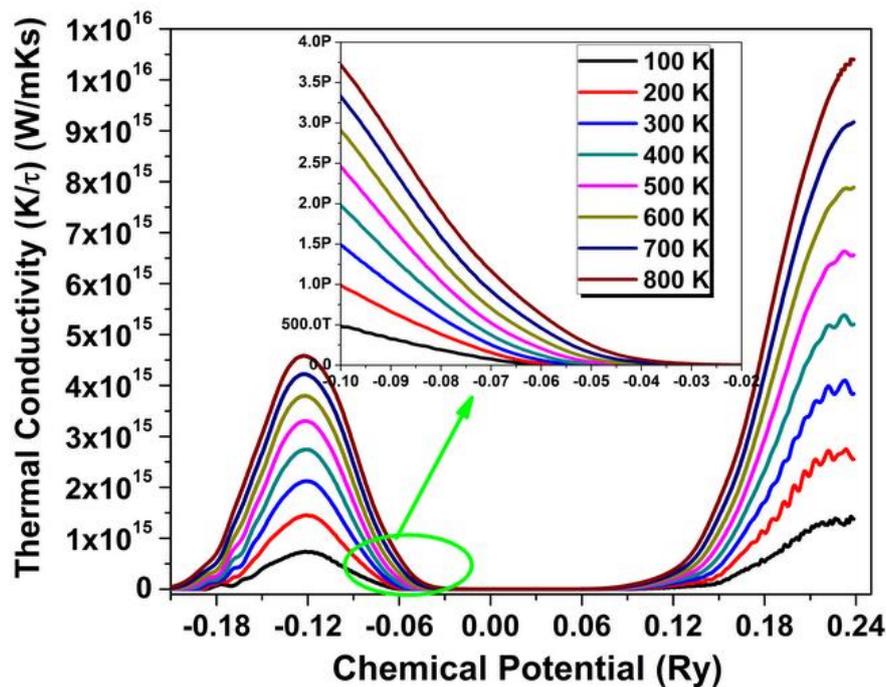
Fig.4: Thermal conductivity of γ-CuI versus chemical potential.

Electrons and phonons are the typical sources of heat conduction in metals and semiconductors respectively and which are account for features of thermal conductivity. Thermal conductivity (K/τ) is an important parameter for TE materials which is the physical quantity of materials to conduct heat. Thermal conductivity of γ-CuI is shown in **Fig.4**. It can be observed that the thermal conductivity gradually increases with the increase of temperature and chemical potential and reaches the maximum value at -0.12 Ry in the p-type doping region. Beyond this region, it decreases exponentially and get minimum values between -0.03 Ry to 0.08 Ry chemical potential. It leads to achieve high figure of merit and it clearly indicates that the present investigated material gives proper TE response in this region. Thermal conductivity rapidly increases with the increase of temperature above the 0.08 Ry chemical potential due to increasing of electrical conductivity and phonon scattering. A large enhancement in the thermal conductivity is observed at 0.23 Ry chemical potential which indicates the absence of phonon conductivity. The observed values of thermal conductivity of γ-CuI are $2 \times 10^{15} W/mKS$ at RT and $4.60 \times 10^{15} W/mKS$ at 800 K. It obviously indicates that the thermal conductivity strongly affects the value of figure of merit.

The electrical conductivity (σ/τ) is another important parameter in the TE performance of TE device. In TE devices, the current is produced as a result of movement of electron from the hot regions of a material to the cold regions. High values of electrical conductivity are necessary for a good TE performance. The calculated anisotropic electrical conductivity of γ-CuI in the temperature range from 100 to 800 K is displayed in **Fig.5**. It shows that the electrical conductivity is increased with the increase of chemical potential and maximum electrical conductivity is observed at -0.12 Ry. The minimum value of electrical conductivity is perceived at in the chemical potential range from -0.06 Ry to 0.08 Ry. The rapid increase in the electrical conductivity is observed above 0.08 Ry chemical potential due to the direct association ofSeebeck co-efficient. The calculated

values of electrical conductivity of γ-CuI are $2.99 \times 10^{20}\,(\Omega mS)^{-1}$ at RT and $2.83 \times 10^{20}\,(\Omega mS)^{-1}$ at 800 K. It is higher than the previously reported values of materials such as $BiGaO_3\,(2.2 \times 10^{18})$, $BiInO_3\,(4.8 \times 10^{18})$[45], ZnO (1.63×10^{18})[46], $CuZnAlS_4\,(1.15 \times 10^{15})$[47] and $Zr_2CoSi\,(5 \times 10^{18})$[48] respectively. The inset figure 5 (a&b) shows the variation of
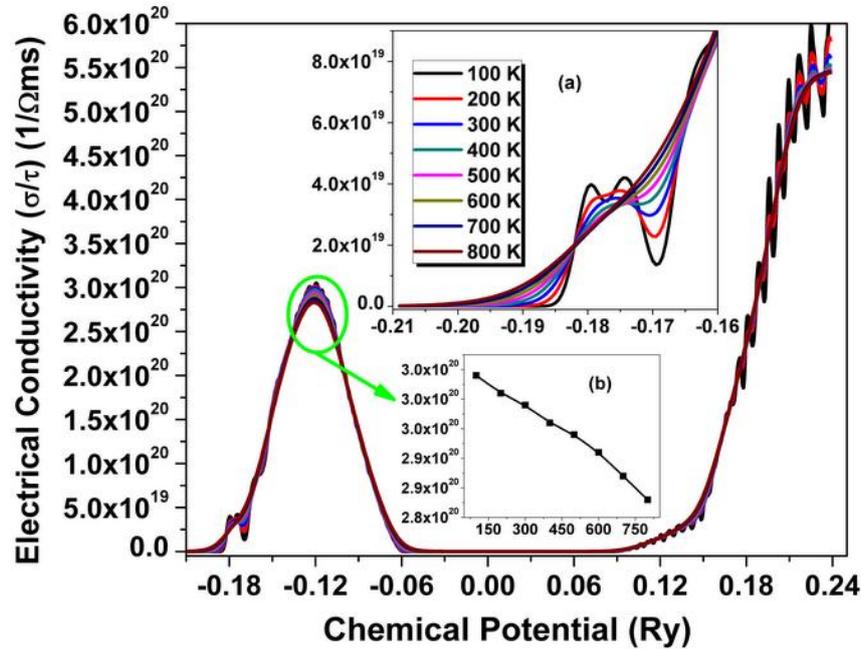
**Fig.5: Electrical conductivity of γ-CuI in the temperature range from 100 to 800 K,
Inset: (a) variation at μ= -0.18 Ry, (b) Electrical conductivity versus temperature**.

electrical conductivity at -0.18 Ry and -0.12 Ry chemical potential. The inset figure 5 (b) depicts change in electrical conductivity with temperature. It can be seen that the electrical conductivity decreases with the increase of temperature which predicts the metallic behaviour of the γ-CuI at -0.12 Ry chemical potential. It is due to the large effective mass by the presence of heavy hole and it is well matched with the results of discussed Seebeckco-efficient.
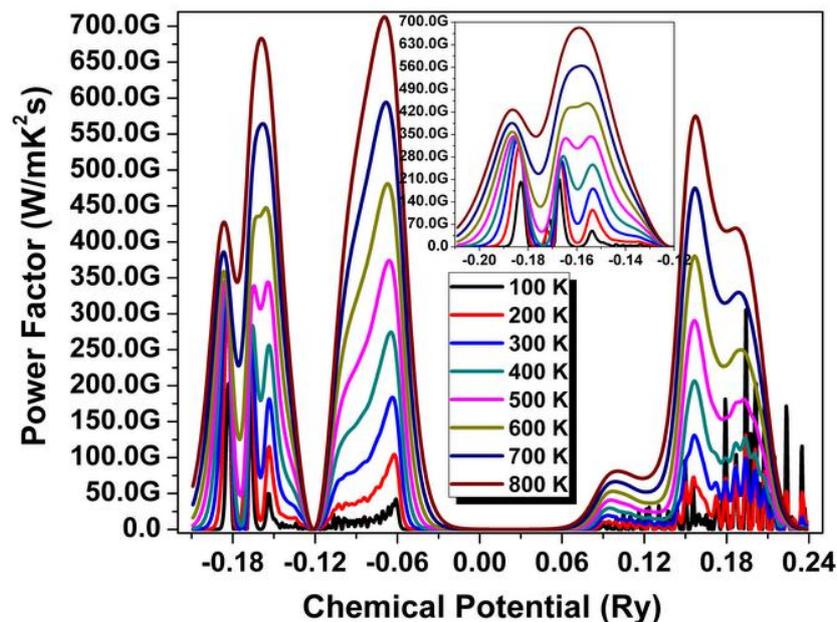
Fig.6: Thermoelectric power factor of γ-CuI for various temperatures.

Power factor ($S^2\sigma/\tau$) is an important parameter gives information about the effectiveness (generation or extraction of heat) of thermoelectric materials. The calculated value of power factor per time of γ-CuI is shown in **Fig.6**. It shows the presence of two peaks in the *p*-type doping and a peak in the *n*-type doping atall temperatures. P-type doping shows higher power factor value than the *n*-type doping because γ-CuI is a *p*-type semiconductor material. Enhancement in the power factor peak values is observed with the increase of temperature from 100 K to 800 K. The maximum power factor value of *p*-type doping is obtained at 717 GW/mK^2S and 575 GW/mK^2S for *n*-type doping of γ-CuI. This high value of power factor forecast the efficient heat generation or extraction of γ-CuI at appropriate doping concentration. It gives the direct information about the doping rangesuggesting that the thermoelectric performance can be enhanced by adopting appropriate doping concentration. It can be further seen that the presence of the optimum power factor values become independent of the chemical potential in the region of the maximum value of the Seebeck co-efficient and electrical conductivity.
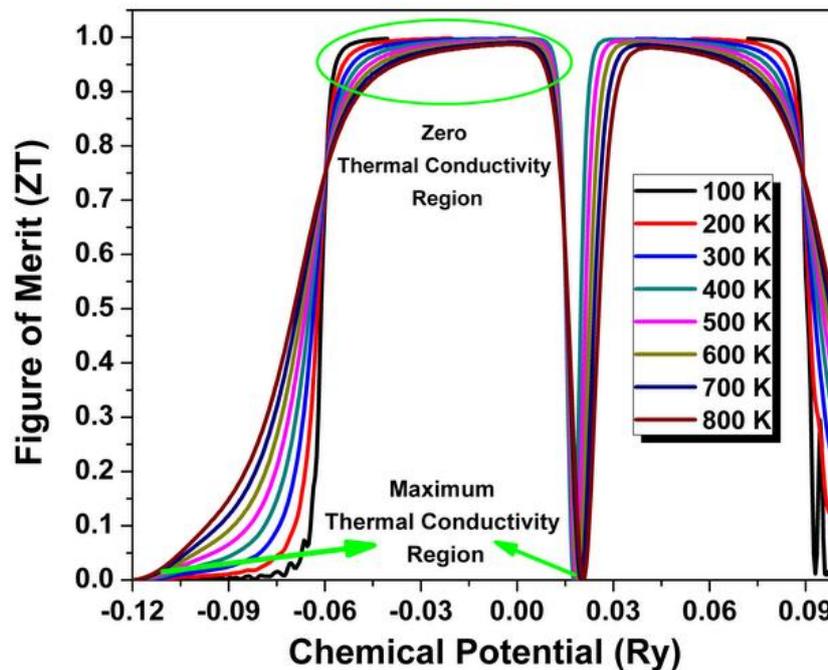
Fig.7: The calculated figure of merit versus chemical potential with various temperatures.

The dimensionless figure of merit plays a vital role in predicting the efficiency of the investigated material for thermoelectric applications and it is calculated mathematically from equation (1). It gives direct information about energy conversion between heat and electricity based on thermoelectric effects without moving parts is an attractive form from any applications in power generation and heat pumping. The calculated figure of merit of γ-CuI as a function of chemical potential is shown in **Fig.7**. The maximum value of figure of merit is observed from 0.8 to 1.0 in the -0.06 to 0Ry (*p*-type doping) chemical potential range for each temperature. A slight decrease is observed with the increase of temperature from 100 K to 800 K whereas it increases from 0 to 0.3 in the p-type (at -0.09Ry) doping region. It is due to the increases/decreases of thermal/electrical conductivity in the γ-CuI for all the temperatures in this region. Besides, the values of the figure of merit are quantitatively equal for the *p*-type and *n*-type doping which is suggest that the γ-CuI can be used as an *p*-type or *n*-type thermoelectric material. It creates very interesting properties for fabricating γ-CuI based thermoelectric devices.

Hence, the more insights into the figure of merit are necessary to discuss as a function of temperature. Therefore, the figure 7 is re-plotted with different optimum chemical potentials and it is presented in **Fig.8**. It can be seen that the figure of merit increases with increase of temperature at 0.032 Ry*p*-type doping while it decreases with increase of temperature for all other doping. However, it lies between 0.84 - 1.0 and it is well accordance
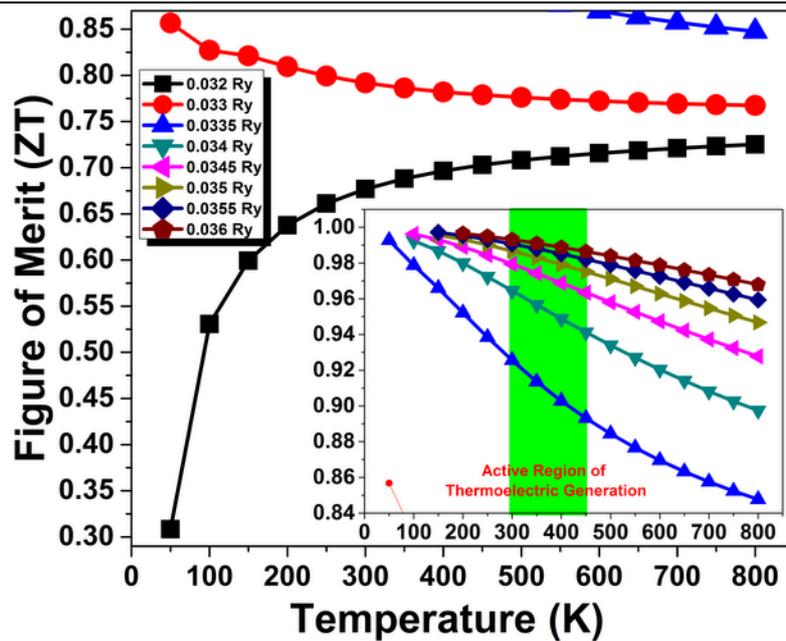
Fig.8: Variation of figure of merit versus temperature with optimum chemical potentials.

with the previous results of different materials [45, 46, 48]. From these results, the active thermoelectric generation region of γ-CuI is found to be 300 K to 450 K range of temperature. The variation of figure of merit with different temperature gradient is presented in **Fig.9**. It clearly depictsthat the increases of temperature gradient leads to an increase of figure of merit which confirms that the γ-CuI act as a very good thermoelectric material.
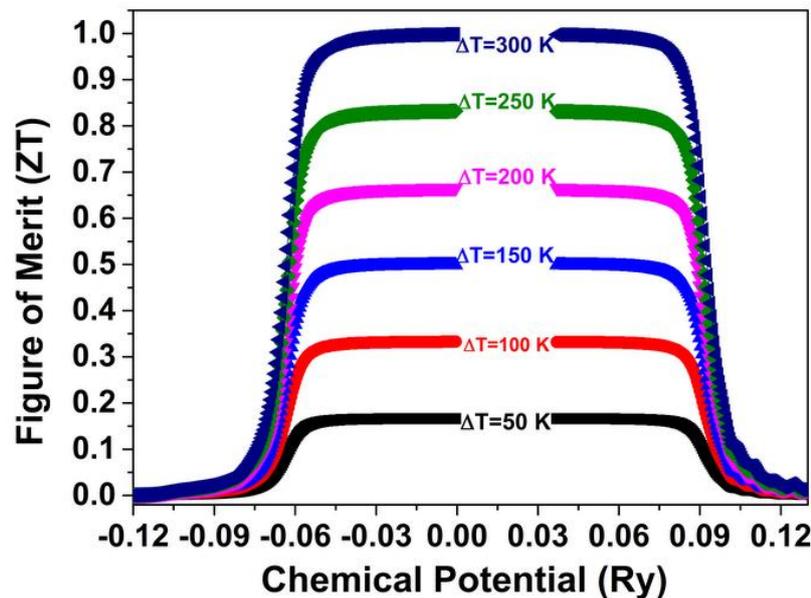
Fig.9: Variation of figure of merit with different temperature gradients.

When a material is subjected to a temperature gradient it would build up a thermoelectric voltage at two ends of the material. It is also directly proportional to the Seebeck co-efficient and the thermoelectric conversion is indirectly connected with the Seebeck co-efficient.Hence, the thermoelectric voltage and conversion efficiency is calculated using the following relation and discussed with respect to Seebeck co-efficient[49, 50].

$$\Delta V = S\Delta T \ \ (V)$$

$$\eta = \frac{\Delta T}{h} \frac{\sqrt{1 + Z\bar{T}} - 1}{\sqrt{1 + Z\bar{T}} + \frac{T_c}{T_h}} \ \ (\%)$$

Where, ΔT is the temperature gradient, T_c and $T_h$are the cold and hot end temperatures, Z is the figure of merit and $\bar{T}$ is the average temperature. Here, we take cold and hot end temperaturesas 300 K and 800 K. The calculated thermoelectric voltage and conversion efficiency is shown in **Fig.10** as a function of Seebeck co-efficient. It exhibits that the thermoelectric voltage increases with the increase of Seebeck co-efficient. The maximum value of thermoelectric voltage is observed at 0.85 V at 283 *mV/K* Seebeck co-efficient. Thermoelectric conversion efficiency is found to decrease with the increase of Seebeck co-efficient. The maximum conversion efficiency value of γ-CuI is 93 % at 138 *mV/K* (800 K) Seebeck co-efficient.
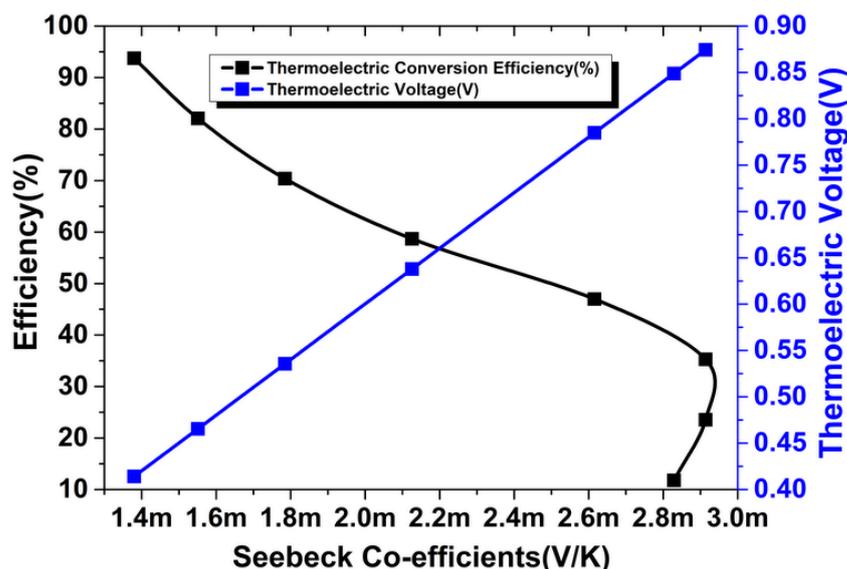
Fig.10: Thermoelectric voltage and conversion efficiency of γ-CuI versus Seebeckco-efficient.

IV. Conclusions

Different thermoelectric properties of γ-CuI are studied using density functional theory contained Boltzmann transport equations. To obtain accurate result, the Tran Blaha modified Becke Johnson potential (TB-mBJ) approximation is used for the exchange correlation potential. P-type semiconductor behaviour of γ-CuI is confirmed from the value of Seebeck co-efficient at zero chemical potential. The large Seebeck co-efficient value observed around $1 - 2.8$ *mV/K* in the $100 - 700$ K temperaturerange on account of large effective mass dominated by heavy hole band. The increases/decreases of thermal/electrical conductivities with respect to the increase of temperature are observed. Enhancement in the power factor peak value with the increase of temperature is observed and maximum power factor (575 *GW/mK²S*) value is found in the p-type doping region. γ-CuI act as a *p*-type/*n*-type thermoelectric material with the presence of quantitatively equal figure of merit (0.8 – 1.0) values in the *p*-type/*n*-type doping region. The calculated thermoelectric voltage and conversion efficiency of γ-CuI is 0.85 V and 93%. From these results, we infer active thermoelectric generation and heat extraction in γ-CuImaterial as observed in the temperature range300 – 450 K which can be used in the fabrication of thermoelectric devices.

Reference

[1]. C. Yang, D. Souchay, M. Kneiß, M. Bogner, H.M. Wei, M. Lorenz, O. Oeckler, G. Benstetter, Y.Q. Fu, M. Grundmann, Transparent flexible thermoelectric material based on non-toxic earth-abundant p-type copper iodide thin film, Nature Communications 8 (2017) 16076.
[2]. R. Venkatasubramanian, E. Siivola, T. Colpitts, B. O'Quinn, Thin-film thermoelectric devices with high room-temperature figures of merit, Nature 413 (2001) 597.
[3]. T.C. Harman, P.J. Taylor, M.P. Walsh, B.E. LaForge, Quantum Dot Superlattice Thermoelectric Materials and Devices, Science 297(5590) (2002) 2229-2232.
[4]. Y. Gelbstein, Phase morphology effects on the thermoelectric properties of Pb0.25Sn0.25Ge0.5Te, Acta Materialia 61(5) (2013) 1499-1507.
[5]. K. Kirievsky, M. Shlimovich, D. Fuks, Y. Gelbstein, An ab initio study of the thermoelectric enhancement potential in nano-grained TiNiSn, Physical Chemistry Chemical Physics 16(37) (2014) 20023-20029.
[6]. Y. Gelbstein, J. Tunbridge, R. Dixon, M.J. Reece, H. Ning, R. Gilchrist, R. Summers, I. Agote, M.A. Lagos, K. Simpson, C. Rouaud, P. Feulner, S. Rivera, R. Torrecillas, M. Husband, J. Crossley, I. Robinson, Physical, Mechanical, and Structural Properties of Highly Efficient Nanostructured n- and p-Silicides for Practical Thermoelectric Applications, Journal of Electronic Materials 43(6) (2014) 1703-1711.
[7]. H. Kawazoe, M. Yasukawa, H. Hyodo, M. Kurita, H. Yanagi, H. Hosono, P-type electrical conduction in transparent thin films of CuAlO2, Nature 389 (1997) 939.

[8]. I. Chowdhury, R. Prasher, K. Lofgreen, G. Chrysler, S. Narasimhan, R. Mahajan, D. Koester, R. Alley, R. Venkatasubramanian, On-chip cooling by superlattice-based thin-film thermoelectrics, Nature Nanotechnology 4 (2009) 235.

[9]. J. Loureiro, N. Neves, R. Barros, T. Mateus, R. Santos, S. Filonovich, S. Reparaz, C.M. Sotomayor-Torres, F. Wyczisk, L. Divay, R. Martins, I. Ferreira, Transparent aluminium zinc oxide thin films with enhanced thermoelectric properties, Journal of Materials Chemistry A 2(18) (2014) 6649-6655.

[10]. V. Brinzari, I. Damaskin, L. Trakhtenberg, B.K. Cho, G. Korotcenkov, Thermoelectrical properties of spray pyrolyzed indium oxide thin films doped by tin, Thin Solid Films 552 (2014) 225-231.

[11]. S. Ohta, T. Nomura, H. Ohta, K. Koumoto, High-temperature carrier transport and thermoelectric properties of heavily La- or Nb-doped SrTiO3 single crystals, Journal of Applied Physics 97(3) (2005) 034106.

[12]. C. Ruttanapun, W. Kosalwat, C. Rudradawong, P. Jindajitawat, P. Buranasiri, D. Naenkieng, N. Boonyopakorn, A. Harnwunggmoung, W. Thowladda, W. Neeyakorn, C. Thanachayanont, A. Charoenphakdee, A. Wichainchai, Reinvestigation Thermoelectric Properties of CuAlO2, Energy Procedia 56 (2014) 65-71.

[13]. K. Hayashi, K.-i. Sato, T. Nozaki, T. Kajitani, Effect of Doping on Thermoelectric Properties of Delafossite-Type Oxide CuCrO2, Japanese Journal of Applied Physics 47(1) (2008) 59-63.

[14]. R. Funahashi, S. Urata, T. Sano, M. Kitawaki, Enhancement of thermoelectric figure of merit by incorporation of large single crystals in Ca3Co4O9 bulk materials, Journal of Materials Research 18(7) (2011) 1646-1651.

[15]. K. Bädeker, Über die elektrische Leitfähigkeit und die thermoelektrische Kraft einiger Schwermetallverbindungen, Annalen der Physik 327(4) (1907) 749-766.

[16]. M. Grundmann, Karl Bädeker (1877–1914) and the discovery of transparent conductive materials, physica status solidi (a) 212(7) (2015) 1409-1426.

[17]. D. Chen, Y. Wang, Z. Lin, J. Huang, X. Chen, D. Pan, F. Huang, Growth Strategy and Physical Properties of the High Mobility P-Type CuI Crystal, Crystal Growth & Design 10(5) (2010) 2057-2060.

[18]. J. Wang, J. Li, S.-S. Li, Native p-type transparent conductive CuI via intrinsic defects, Journal of Applied Physics 110(5) (2011) 054907.

[19]. K. Tennakone, G.R.R.A. Kumara, I.R.M. Kottegoda, V.P.S. Perera, G.M.L.P. Aponsu, K.G.U. Wijayantha, Deposition of thin conducting films of CuI on glass, Solar Energy Materials and Solar Cells 55(3) (1998) 283-289.

[20]. [20] J. Zhu, M. Gu, R. Pandey, Structural and electronic properties of CuI doped with Zn, Ga and Al, Journal of Physics and Chemistry of Solids 74(8) (2013) 1122-1126.

[21]. M. Xia, M. Gu, X. Liu, B. Liu, S. Huang, C. Ni, Electrical and luminescence properties of Zn2+ doped CuI thin films, Journal of Materials Science: Materials in Electronics 26(4) (2015) 2629-2633.

[22]. C. Yang, M. Kneiß, M. Lorenz, M. Grundmann, Room-temperature synthesized copper iodide thin film as degenerate p-type transparent conductor with a boosted figure of merit, Proceedings of the National Academy of Sciences 113(46) (2016) 12929.

[23]. [23] M.K. Yadav, B. Sanyal, First-principles study of thermoelectric properties of CuI, Materials Research Express 1(1) (2014) 015708.

[24]. P. Blaha, WIEN 2 k, An Augmented Plane Wave+Local Orbitals Program for Calculating Crystal Properties (2001).

[25]. J.P. Perdew, K. Burke, M. Ernzerhof, Generalized Gradient Approximation Made Simple, Physical Review Letters 77(18) (1996) 3865-3868.

[26]. F. Tran, P. Blaha, Accurate Band Gaps of Semiconductors and Insulators with a Semilocal Exchange-Correlation Potential, Physical Review Letters 102(22) (2009) 226401.

[27]. R. Vettumperumal, J.R. Jemima, S. Kalyanaraman, R. Thangavel, Analysis of electronic and optical properties of copper iodide (γ-CuI) by TB – mBJ method – A promising optoelectronic material, Vacuum 162 (2019) 156-162.

[28]. G.K.H. Madsen, D.J. Singh, BoltzTraP. A code for calculating band-structure dependent quantities, Computer Physics Communications 175(1) (2006) 67-71.

[29]. J. Ziman, Electrons and phonons : the theory of transport phenomena in solids, Clarendon Press, Oxford, 2001.

[30]. X. Gao, K. Uehara, D.D. Klug, S. Patchkovskii, J.S. Tse, T.M. Tritt, Theoretical studies on the thermopower of semiconductors and low-band-gap crystalline polymers, Physical Review B 72(12) (2005) 125202.

[31]. L. Chaput, P. Pécheur, J. Tobola, H. Scherrer, Transport in doped skutterudites: Ab initio electronic structure calculations, Physical Review B 72(8) (2005) 085126.

[32]. G.K.H. Madsen, Automated Search for New Thermoelectric Materials: The Case of LiZnSb, Journal of the American Chemical Society 128(37) (2006) 12140-12146.

[33]. D. Parker, D.J. Singh, Thermoelectric properties of AgGaTe${}_{2}$ and related chalcopyrite structure materials, Physical Review B 85(12) (2012) 125209.

[34]. J. Zhu, R. Pandey, M. Gu, The phase transition and elastic and optical properties of polymorphs of CuI, Journal of Physics: Condensed Matter 24(47) (2012) 475503.

[35]. B. Bouhafs, H. Heireche, W. Sekkal, H. Aourag, M. Certier, Electronic and optical properties of copper halides mixed crystal CuCl1−xIx, Physics Letters A 240(4) (1998) 257-264.

[36]. X. Chen, D. Parker, M.-H. Du, D.J. Singh, Potential thermoelectric performance of hole-doped Cu2O, New Journal of Physics 15(4) (2013) 043029.

[37]. Y. Pei, X. Shi, A. LaLonde, H. Wang, L. Chen, G.J. Snyder, Convergence of electronic bands for high performance bulk thermoelectrics, Nature 473 (2011) 66.

[38]. A.F. Ioffe, Semiconductor thermoelements, and Thermoelectric cooling, Infosearch, London, 1957.

[39]. S.-W. Kim, Y. Kimura, Y. Mishima, High temperature thermoelectric properties of TiNiSn-based half-Heusler compounds, Intermetallics 15(3) (2007) 349-356.

[40]. D.J. Singh, Doping-dependent thermopower of PbTe from Boltzmann transport calculations, Physical Review B 81(19) (2010) 195217.

[41]. C. Wood, Materials for thermoelectric energy conversion, Reports on Progress in Physics 51(4) (1988) 459-539.

[42]. D.M. Rowe, CRC handbook of thermoelectrics, CRC Press, Boca Raton, FL, 1995.

[43]. K. Nishikawa, Y. Takeda, T. Motohiro, Thermoelectric properties of molten Bi2Te3, CuI, and AgI, Applied Physics Letters 102(3) (2013) 033903.

[44]. C. Herring, Theory of the Thermoelectric Power of Semiconductors, Physical Review 96(5) (1954) 1163-1187.

[45]. Rasul B. Behram, M.A. Iqbal, S.M. Alay-e-Abbas, M. Sajjad, M. Yaseen, M.I. Arshad, G. Murtaza, Theoretical investigation of mechanical, optoelectronic and thermoelectric properties of BiGaO3 and BiInO3 compounds, Materials Science in Semiconductor Processing 41 (2016) 297-303.

[46]. P. Sikam, C. Sararat, P. Moontragoon, T. Kaewmaraya, S. Maensiri, Enhanced thermoelectric properties of N-doped ZnO and SrTiO3: A first-principles study, Applied Surface Science 446 (2018) 47-58.

[47]. Thermoelectric properties of stannite-phase CuZn2AS4 (CZAS; A=Al, Ga and In) nanocrystals for solar energy conversion applications AU - Yalcin, Battal Gazi, Philosophical Magazine 96(21) (2016) 2280-2299.
[48]. S. Yousuf, D.C. Gupta, Chemical Potential Evaluation of Thermoelectric and Mechanical Properties of Zr2CoZ (Z = Si, Ge) Heusler Alloys, Journal of Electronic Materials 47(4) (2018) 2468-2478.
[49]. G.J. Snyder, T.S. Ursell, Thermoelectric Efficiency and Compatibility, Physical Review Letters 91(14) (2003) 148301.
[50]. J. Martin, T. Tritt, C. Uher, High temperature Seebeck coefficient metrology, Journal of Applied Physics 108(12) (2010) 121101.